The relation between galaxy morphology and merger history in the EAGLE simulations

THESIS

submitted in partial fulfillment of the
requirements for the degree of

MASTER OF SCIENCE
in
ASTRONOMY AND RESEARCH

Author :	Malavika Vijayendra Vasist
Student ID :	s2033046
Supervisor 1:	Joop Schaye
Supervisor 2:	Camila Correa

Leiden, The Netherlands, June 2018

The relation between galaxy morphology and merger history in the EAGLE simulations

Malavika Vijayendra Vasist

Leiden Observatory, Leiden University
P.O. Box 9500, 2300 RA Leiden, The Netherlands

June 2018

Abstract

We investigate the link between merger history of galaxies, stellar mass and galaxy morphology using the EAGLE cosmological hydrodynamical simulations. We define the stellar mass of a galaxy as the total stellar mass within 30kpc, quantify galaxy morphology using a kinematic-based parameter kappa-corotating and map the distribution of ellipticals and disks across redshifts in the simulation. We consider galaxy pairs within a certain spatial proximity to be impending merger events and differentiate them as major or minor depending on the ratio of the masses of the galaxies comprising it. The contribution of major mergers in the evolution of galaxies is estimated by the fraction of galaxies in close pairs, namely the fraction of major mergers (fMM). fMM reveals that the probability of major mergers is independent of stellar mass but depends on morphology, with fMM being higher for ellipticals than disks at all redshifts, agreeing with recent observational estimates. We also find that independent of morphology, the probability of mergers increases with the increase in redshift. To understand the morphological composition of galaxies in close pairs, we calculate the fraction of the pairs constituting galaxies belonging to the same morphology. We find that the probability of finding two elliptical galaxies merging is higher than finding two disk type galaxies.

Contents

Version of June 2018– Created August 1, 2018 - 11:03

List of Figures

Chapter 1

Introduction

Galaxies are gravitationally bound structures in the Universe comprising star, interstellar gas, dust and dark matter particles that rotate around its centre of potential. Based on visual inspection, we know that galaxies exist in various morphologies that can be broadly classified as ellipticals, lenticulars, spirals and irregulars. Ellipticals, as the name suggests looks like an ellipse. They have a central bulge that comprise random stellar motions. They are characterised by a collective slow rotation about the centre. Spirals on the other hand have a smaller bulge at the centre and a bigger flattened disk that is comprised of stars, dust and gas rotating in a fast and orderly manner. They also have spiral arms that originate from centre and extend upto the edge of this galactic disk. Lenticulars have characteristics midway between ellipticals and spirals as they have both a well defined bulge and a disk at the centre. They are classified under ellipticals in most cases. Lastly, irregular galaxies are mostly galaxies that dont have any shape.

How these galaxies evolved to assume their respective galactic properties like morphology, mass and size is yet to be answered. Galaxy evolution is quantified by changes to these properties which can occur either due to in-situ factors via 'disk instabilities' (Kormendy Kennicutt. 2004) or external factors like 'mergers'. According to the standard model of galaxy formation (Fall and Efstathiou. 1980 and Mo,Mao and White. 1998), as gas cools down in bubbles of dark matter haloes, they do so along flat disks forming disk-like galaxies. They rotate at high speeds and eventually develop spiral arms. This orderly rotation of stars around the centre of potential of galaxies is disrupted by mutual interactions or mergers, and as a consequence lead to a morphological transformation from disks to slow moving elliptical galaxies also growing in their size and mass. To understand how significant mergers are in causing this morphological transformation, we study how galaxy merger history relates with morphology in the EAGLE simulations.

Version of June 2018– Created August 1, 2018 - 11:03

1.1 Impact of mergers on galaxy evolution

A galaxy undergoes a merger when it collides with another galaxy. In literature the effect of mergers on galactic properties have been explored by means of both observations and simulations. Analysis of central galaxies in EAGLE simulations have shown that major mergers (where galaxy mass ratio $\mu = 1/4$) are responsible for most mass growth in massive galaxies ($11 < \log_{10}M[M\odot] < 12$) mostly due to the accretion of ex-situ stars (stars formed outside the halo of the galaxy) and very little in-situ star formation (Qu et al. 2016). It is seen that this accretion of ex-situ stars at large radii also causes the build up of spheroids that stand out more than the disks and lead to a morphological transformation from disk-like morphology to a spheroid-like morphology in more massive ($\log_{10}M[M\odot] > 10.5$) galaxies (Clauwens et al. 2018). This morphological transformation is seen in gas-poor mergers (mergers of galaxies with low gas-to-stellar mass ratio), whereas it is seen that gas-rich mergers trigger in-situ star formation that contributes towards disk retention (Rodriguez-Gomez et al. 2017- Illustris), hence making mergers inefficient in destroying disks (Kannan et al. 2015- Horizon-AGN). Therefore, gas-poor mergers are also known to reduce the angular momentum of the galaxies whereas the gas-rich ones increase it (Lagos et al. 2017- EAGLE simulations).

MUSE (Deep Multi Unit Spectroscopic Explorer- Ventou et al. 2017) uses observations in the Hubble Ultra Deep Field (HUDF) and Hubble Deep Field South (HDF-S) to evaluate the significance of mergers by mapping the evolution of the fraction of pairs with respect to the galaxy population per redshift (as in Qu et al. 2016). It is seen that mergers increase till redshift three and then reduce. This might imply that mergers are linked to the cosmic star formation rate evolution where most morphological transformations occur (eg. Madau Dickinson. 2014).

All the above stated simulations and the observation suggest that mergers are important in shaping the evolution of galaxies. Since their significance correlates with how often they occur, in this thesis we calculate their occurrence with respect to the galaxy population in EAGLE.

1.2 EAGLE simulations

Simulations form an important aspect of modern day research. This is because with simulations we can verify the understanding of underlying physical processes in cosmic systems by comparing simulation results with observational results. Once verified, simulations can be helpful in understanding the evolution of systems which is otherwise harder to gather just from observational results as the Universe operates on a way bigger timescale than an average human lifetime.

The simulations used here are the EAGLE simulations(McAlpine et al. 2016 and The EAGLE team 2017). EAGLE stands for Evolution and Assembly of Galaxies and their Environments. This simulates the evolution of dark matter, gas, stars from redshift z=127 to present day at z=0. It is based on the

Version of June 2018– Created August 1, 2018 - 11:03

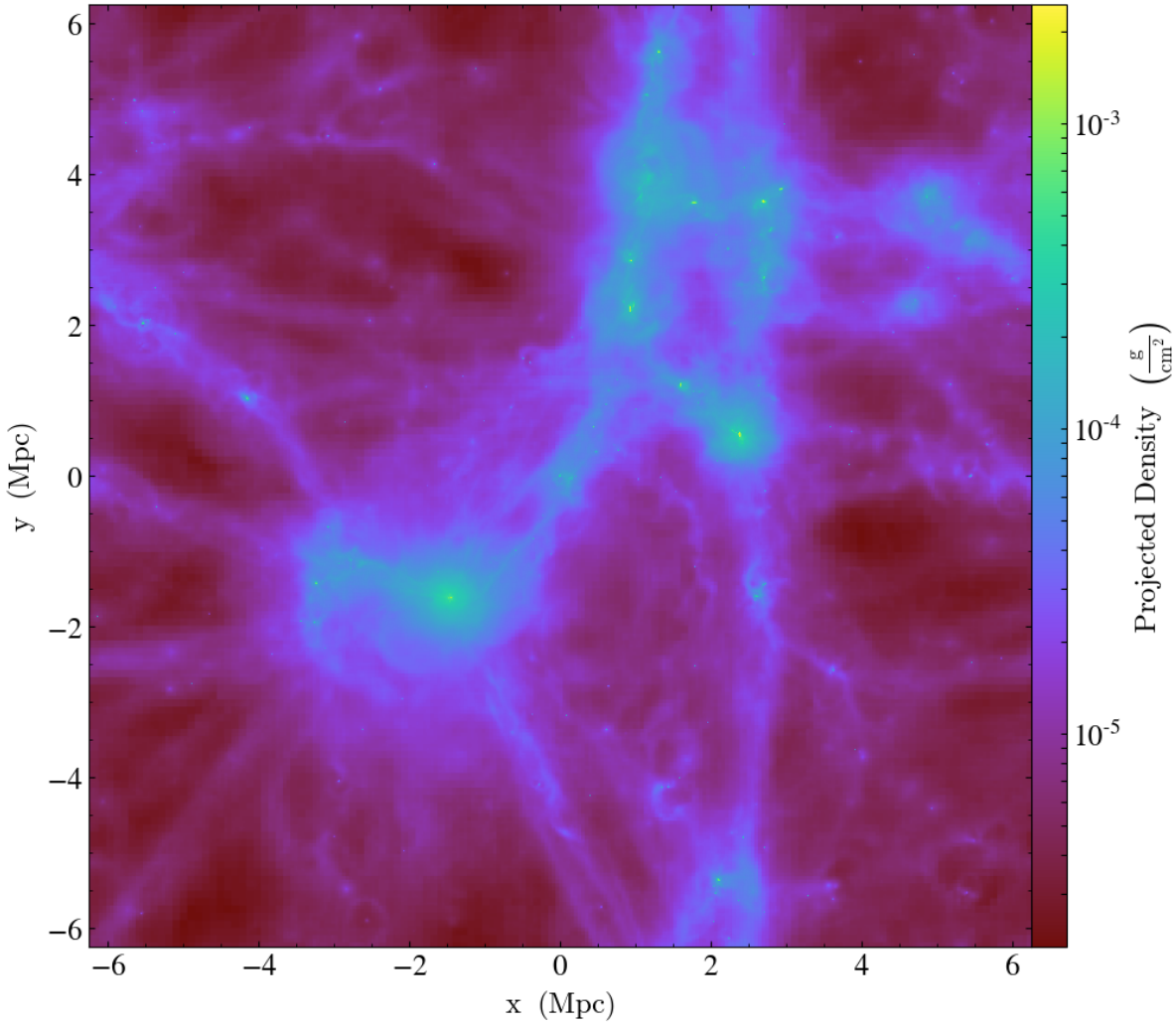

Figure 1.1: *What we see is the visualization of EAGLE. A density plot of all the particles in the simulation L0012N0188 within a box of length 12 Mpc at redshift zero is plotted here. Image Courtesy: Dr Camila Correa, Leiden University.*

ΛCDM cosmology with parameters derived from the data of Planck Collaboration (2014). The code used to carry this out is a modified version of the parallel N-body smoothed particle hydrodynamics (SPH) GADGET 3 code (Springel et al. 2008; Springel 2005). The modifications done to the SPH solver that EAGLE uses are termed as Anarchy.

EAGLE uses several physics subgrid modules in an attempt to capture the physics realistically, namely- radiative cooling and photo-heating (Wiersma, Schaye and Smith 2009), star formation (Schaye and Dalla Vecchia 2008), stellar evolution and enrichment (Wiersma et al 2009), blackhole growth (Springel et al. 2005; Rosas- Guevara et al. 2015) and Stellar and AGN feedback (Dalla Vecchia Schaye 2012). The parameters for these modules are calibrated with values that fit with observations.

The simulation starts with a fixed number of DM particles. An algorithm called the 'Friends-of-Friends' (FoF) algorithm (Davis et al 1985) is used to identify bound structures of DM particles. This algorithm considers all the DM particles closer than 0.2 times the mean DM distance to be in the same clump called a 'halo'. Once DM clups are identifed, all baryonic structures that are gravitationally bound are identified within the halo through an algorithm called SUBFIND algorithm (Springel et al 2001; Dolag et al 2009). These structures are called 'subhaloes'. Most subhaloes in EAGLE contain galaxies. The centre of each of the subhalo is defined by the local minima in the gravitational potential field. The subhalo with the lowest minimum compared to all other subhaloes in the halo is considered the main subhalo. The galaxy in the main subhalo is defined as the 'central galaxy'. The rest of the galaxies in the halo are classified as 'satellites'.

Of the several simulations of various cosmological volumes and resolutions run by EAGLE, this thesis uses the reference model, Ref-L100N1504 run in a co-moving box of size 100 cMpc comprising of an equal number (1504^3) of gas and dark matter particles in the beginning of the simulation where the gas and dark matter(DM) particles have a mass of 1.81×10^6 $M_\odot$ and 9.7×10^6 $M\odot$ each respectively. The simulation also assumes a softening length of 0.7 proper kpc.

As the simulation progresses, the state of the system is stored at 29 time instants (snapshots) from z=20 to z=0. The simulation is also stored in several smaller time intervals called snipshots. There are 200 snipshots between redshifts z=20 to z=0. This allows for a higher time resolution and inturn a more nuanced analysis of the time evolution of galaxies and their properties. This thesis is aimed at exploring what the higher resolution of the simulation can reveal about galaxy and its morphological evolution. The table below shows the parameters of the simulation used here.

Parameter	units	value
box length	cMpc	100
# of particles		2×1504^3
gas particle mass	$M\odot$	1.81×10^6
DM particle mass	$M\odot$	9.7×10^6

Fig. 1.1 visualises EAGLE simulations. This is a density plot of all the particles in the simulation L0012N0188 within a box of length 12 Mpc at redshift zero.

This composite image is produced using projection in the z direction. 'friends of friend' (FoF) algorithm is used to simulate the dark matter clusters, and a 'subfind' algorithm is used to fill them up with baryonic particles based on which DM particles (within a cluster) they are gravitational bound to. The color scale shows the variation of density in the plot. The bright green spots seen here are the most dense regions of the simulation. This plot is centered at the maximum potential.

1.3 Sample Space

The stellar mass of a galaxy is defined as the mass from all of its stars that lie within a 30kpc radius (to match observations) from its centre of potential. The extent of the galaxy is defined in terms of its half mass radius (HMR) which is the distance at which half the galaxy mass is enclosed. In this thesis we focus on galaxies that are more massive than $10^{9.5}$ M$\odot$. Since each star particle has a mass of 1.81×10^{6} M$\odot$, this threshold corresponds to 1000 star particles hence preventing any resolution effects. There are 7421 galaxies in this mass range at redshift zero. As galaxies evolve, this changes with time/redshift.

1.4 This thesis

In this thesis, we explore the link between merger history and galaxy morphology and also comment on the environment of galaxies in EAGLE simulations.

In Chapter 2, we define major mergers for a fixed value of mass criteria and several values of distance criteria. We calculate the fraction of the galaxies that are in major pairs, as the fraction of major mergers (fMM). We show that fMM is independent of stellar mass at redshift zero, and map its evolution through time. We find that fMM increases with an increase in redshift. For each definition of major mergers we compare the corresponding values of the fraction of major mergers (fMM) with observation studies from MUSE (E.Ventou et al. 2017) and Qu et al. (2016), and pick appropriate values of distance and mass criteria for further analysis. By doing so we obtain a distance criteria of 30kpc and a mass criteria (μ) of 1/6. We show the effect of using projection rather than 3D estimations and perform further analysis as an observer would.

In Chapter 3, we classify galaxies as disks and ellipticals according to a kinematic based parameter called kappa-corotating (κ_{corot}). We map the distribution of disks and ellipticals at redshift zero and find that low and high mass galaxies are mostly elliptical whereas moderately massive galaxies are disks and show that this result agrees with Martin et al. (2017) and Clauwens et al. (2018). We conclude that there are more elliptcals than disks at redshift zero, agreeing with Martin et al. (2017). We compare two different models of galaxy evolution and explore what our results suggest. The evolution of morphology of galaxies through time finds that the number of ellipticals dominate at redshifts higher than one. We calculate the fraction of major mergers (fMM) for ellipticals and disks and conclude that the probability of experiencing a merger

Version of June 2018– Created August 1, 2018 - 11:03

is higher for ellipticals than disks at all redshifts. We explore the morphological composition of pairs and arrive at a conclusion that most mergers involve at-least one elliptical galaxy. We plot the cumulative fMM through time to understand the how mergers have shaped galaxies in the local universe and conclude that mergers are rare and not entirely responsible for the morphological transformation of galaxies.

Chapter 2

Fraction of major mergers (fMM)

In this chapter, we define major mergers with a fixed mass criteria and several values of distance criteria, and compare the corresponding fraction of major mergers (fMM) to the observation studies from MUSE. Based on this comparison, we pick an appropriate value for the distance criteria and use it for all further analysis. We apply projection to analyse data just as an observer would.

2.1 Defining major mergers

We define mergers by applying the technique of 'close pairs'. We believe that spatially close galaxies are gravitationally bound to each other and are eventually destined to collide. This makes close pairs a good estimate of mergers. We arrive at an appropriate proximity threshold, the distance criteria, to identify close pairs. Once close pairs are identified, they are considered as mergers and classified as 'major' or 'minor' depending on the ratio of the masses of the galaxies constituting the pair. If the galaxy under consideration (M_1) is in close pairing with a neighbouring galaxy (M_2) and their mass ratio μ (Mu) = M_2/M_1 where $M_1 > M_2$, is greater than a predefined mass criteria of $1/6$, it is considered to be a major merger. Hence, any two galaxies that lie within the distance criteria and has a mass ratio greater than the mass criteria of $1/6$, is considered be to a major merger.

In an effort to choose an appropriate distance criteria, we start by mapping the distribution of sizes of all the galaxies in the simulation versus its mass in Fig. 2.1. We quantify the size of a galaxy by its half mass radius (HMR), defined as the distance from its centre of potential encompassing half the stellar mass of the subhalo that the galaxy is in. From the Fig. 2.1, we find that most of the galaxies have a HMR within 30kpc. Hence, we make a preliminary estimation that a good proximity threshold for two galaxies to be deemed close pairs must

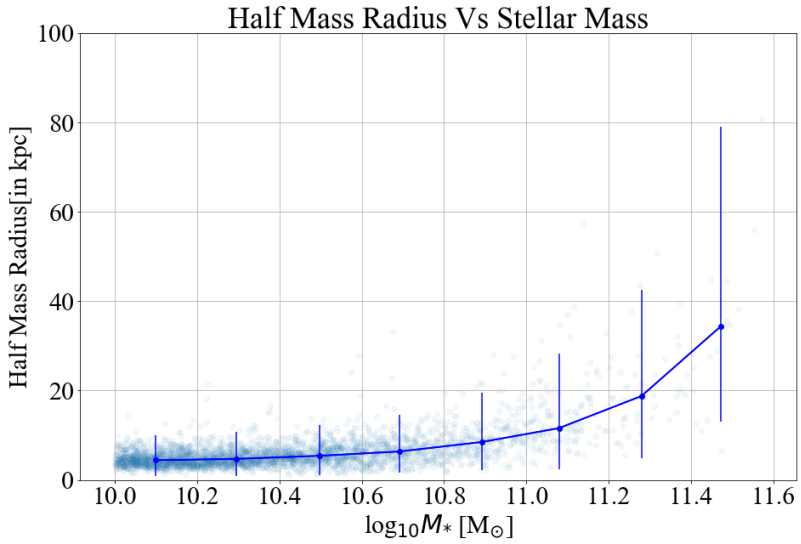

Figure 2.1: *Half Mass Radius is plotted against Stellar Mass for all the galaxies of the simulation. The error bars signify 25 and 75 percentiles. It can be seen that much of the galaxies have a HMR less than 30kpc hence making it a good proximity threshold to identify close pairs.*

be in the distance range of 30kpc and above. The figure is plotted with error bars indicating the 25th and 75th percentiles. It is seen that the HMR scattering increases with the increase in the stellar mass of the galaxies. In all, we observe that the size of a galaxy increases with increasing stellar mass.

2.2 Fraction of Major Mergers (fMM)

The contribution of major mergers in galaxy evolution is understood in terms of the number of merger events that occur through time. This is estimated in terms of a parameter that calculates the fraction of all galaxies that are in major pairs called the 'fraction of Major Mergers'; hereafter fMM.

The fMM is defined as the ratio of the total number of major pairs to the total number of galaxies in the sample space. fMM depends on how the major mergers are defined which are inturn defined by a specific distance and mass criterion as stated in the previous section. To understand to what extent a chosen distance criteria affect the conclusions drawn, we explore different values for the same and compare their corresponding values of fMM. We then select the most appropriate distance criteria and use it for the rest of the analysis. Here, we take the mass criteria to be 1/6 (E.Ventou et al. 2017).

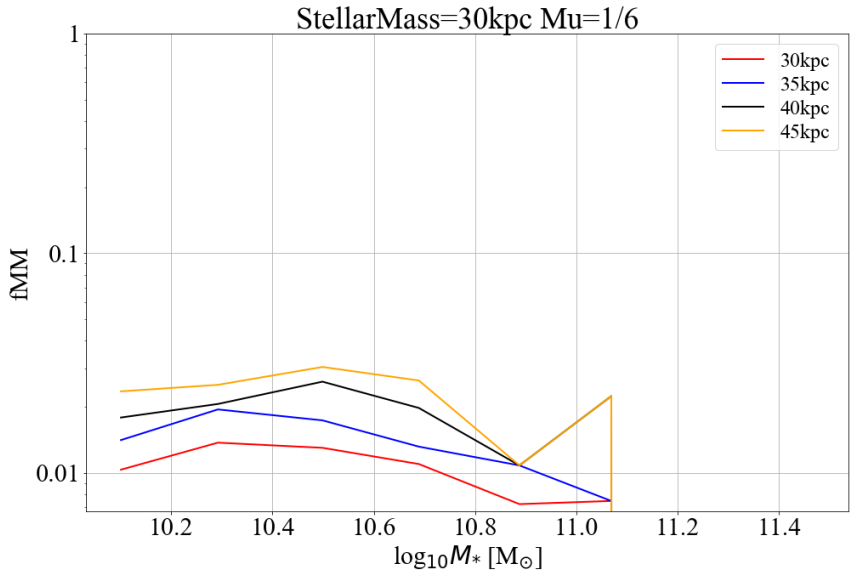

Figure 2.2: *The fraction of Major Mergers (fMM) is plotted against Stellar Mass at redshift 0. The fMM is independent of the Stellar Mass.*

2.2.1 Fraction of Major Mergers at Redshift zero

At redshift zero, we plot the fMM versus the median value of the stellar mass of the galaxies in each bin. Here, the fraction of Major Mergers(fMM) is defined as-

$$fMM = \frac{number\ of\ major\ pairs}{total\ number\ of\ galaxies\ in\ the\ mass\ bin}$$

Different Criteria compared

We compare the fMM as a function of stellar mass as defined above, using two types of distance criteria, namely fixed and flexible type shown in 2.2 and Fig. 2.3 respectively. The fixed distance criteria is defined by constant proper distances beyond 30kpc (30-45kpc) and the flexible distance criteria is defined by various multiples of the half mass radius (3-7 HMR).

We see in Fig. 2.2 that with a fixed distance criteria the fMM is independent of stellar mass whereas in Fig. 2.3 we see that with a flexible distance criteria, the fMM increases with increasing stellar mass. These discordant results can be resolved by further inspection. From Fig. 2.1, we see that massive galaxies have a higher HMR, which implies that they have a bigger search radius that accounts for more pairs than less massive galaxies, thus making their fMM higher than less massive galaxies. This might be the reason why we see an increase in fMM with the increase in stellar mass with a flexible distance criteria. Therefore

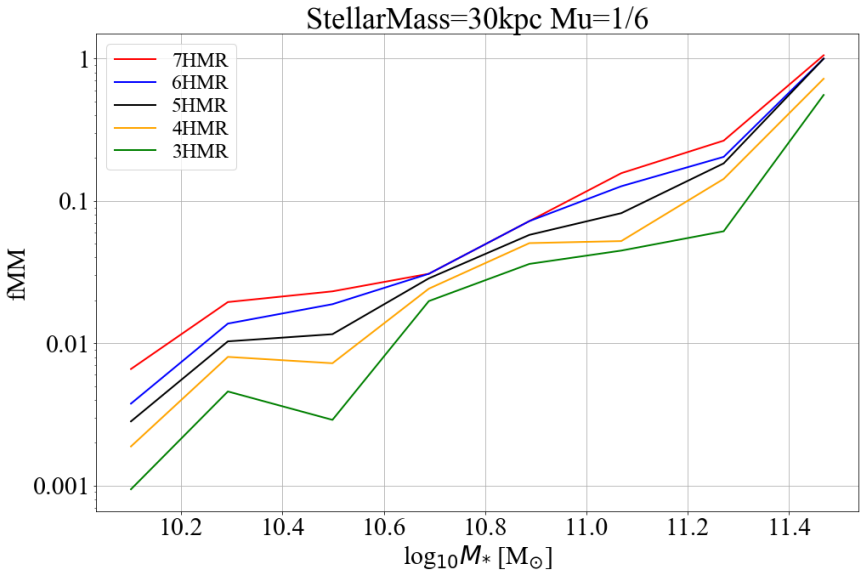

Figure 2.3: *The fraction of Major Merger (fMM) is plotted against Stellar Mass at redshift zero. This increase in the fMM with Stellar Mass is due to the flexible distance criteria used to calculate the fMM. Since HMR for more massive galaxies is larger than for less massive ones, it accounts for more number of pairs hence having an increased fMM.*

on acknowledging this, we conclude that fMM must be independent of stellar mass. We see that this association between the search radius and fMM is more evident in the way the fMM increases as the distance criteria within each type considered (fixed and flexible) increases.

Similarly, different mass criteria, namely, $\mu = 1/6$th and $\mu = 1/4$th, were used, and their corresponding fMM were compared. It was seen that the fMM slightly decreased as the mass criterion was increased from 1/6th to 1/4th as it accounted for less number of major pairs, but the overall trend was maintained.

2.2.2 Evolution of fraction of major mergers through redshifts

We carry out the same analysis as above for all redshifts. Here, the fraction of Major Mergers (fMM) is defined as -

$$fMM = \frac{number\ of\ major\ pairs\ in\ a\ redshift}{total\ number\ of\ galaxies\ in\ that\ redshift}$$

We calculate the fMM for a mass criteria $\mu = 1/6$ and three different distance criteria namely 30kpc, 100kpc and 7HMR across all redshifts. This is plotted in dotted lines across all redshifts along with a bold line plot (or the trend) of fMM versus the median of redshifts in each redshift bin of binsize 0.2 in Fig. 2.4. We find that, the fMM increases continuously for a distance criteria of 30kpc. It increases till redshift 1 and stays constant for all higher redshifts for a distance

criteria of 100kpc and reduces with an increase in redshift for a distance criteria of7HMR.

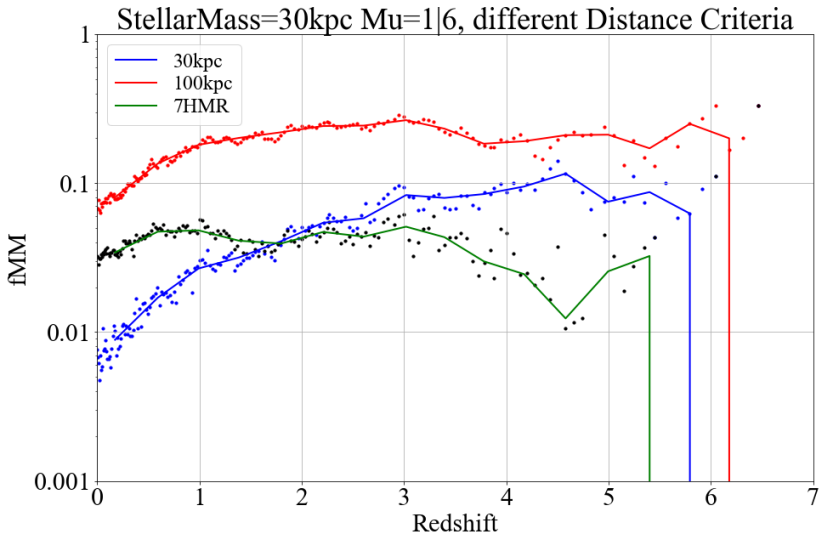

Figure 2.4: *Fraction of major mergers as a function of redshift for a distance criteria of 30kpc, 100kpc nad 7HMR as indicated in the legends. fMM increases continuously, stays constant and reduces with an increase in redshift for distance criteria 30kpc, 100kpc and 7HMR respectively.*

2.3 Comparing with observations

MUSE (Deep Multi Unit Spectroscopic Explorer) are observations conducted in the Hubble Ultra Deep Field (HUDF) and Hubble Deep Field South (HDF-S), to identify close pairs because close pairs are believed to be merging based on their interacting features. Its sample space includes all galaxies with a measured spectroscopic redshift from the fields HDF-S, udf-10 and UDF- Mosaic. This comprises 1801 galaxies that spread over a redshift range of 0.2 to 6 with stellar masses ranging from $7 < \log_{10} M[M\odot] < 11$. 113 close pairs are identified based on the projected distance limit of 25 h^{-1} kpc and a relative velocity of 500 km/s. These pairs are also validated by spectroscopic means. The fraction of major mergers for a redshift bin is defined as the ratio of number of close pairs to the number of primary galaxies in the parent sample (along with several correction factors considered to account for the inadequate spacial resolution, imperfect accuracy in redshift measurements and exclusion of galaxies in the border of the MUSE filed).

We compare the trend of fMM shown in Fig. 2.4 with observations from MUSE (from Ventou et al. 2017) for distance criteria 30kpc, 100kpc and 7HMR plotted in figures 2.5, 2.6 and 2.7 respectively. The MUSE observations calculates

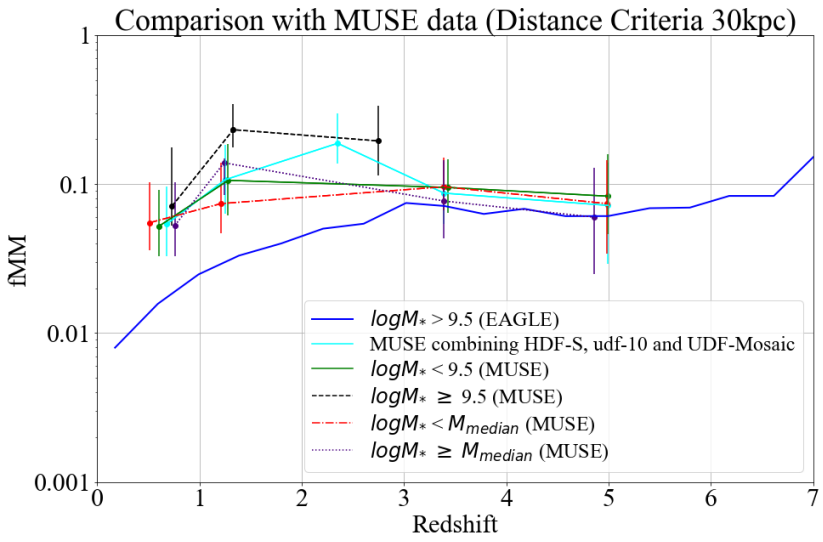

Figure 2.5: *Comparing MUSE data with EAGLE for a Distance Criteria of 30kpc*

the fMM separately for galaxies that are less massive than and more massive than $10^{9.5}[M\odot]$ and the corresponding median value of the stellar mass of the galaxies in pairs within each redshift bin.

It is seen from the comparisons that a distance criteria of 100kpc over-estimates the fraction of Major Mergers (fMM) whereas a distance criteria of 7HMR under-estimates it. A distance criteria of 30 kpc agrees with the observations fairly well. This bolsters the usage of 30kpc as the distance criteria for all further analysis.

We also compare Fig. 2.4 to Fig. 9 of Qu et al. (2016). The paper classifies two galaxies as a merging pair, if they are separated by a distance less than 5 times the half stellar mass radius of the galaxy considered; have a mass ratio greater than 1/4 (less massive to more massive) and share a common future descendant in the EAGLE simulations. It defines the galaxy merger fraction as the ratio of the number of galaxies that are in pairs to the total number of galaxies in that snapshot. The plot of major merger fraction as a function of redshift for galaxies binned in stellar mass is shown in Fig. 9 of Qu et al. (2016). We conclude that this corroborates our results as we see that the major merger fraction increases with redshift and levels at redshift three till redshift four.

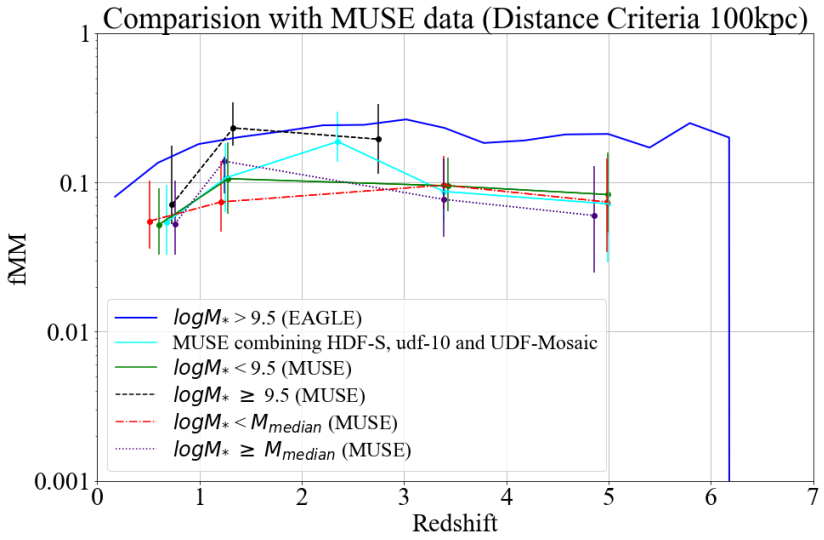

Figure 2.6: *Comparing MUSE data with EAGLE for a Distance Criteria of 100kpc*

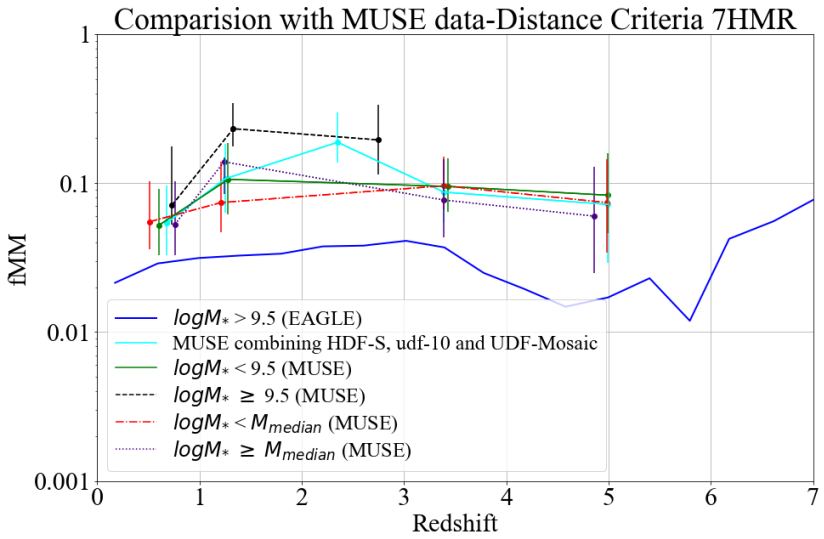

Figure 2.7: *Comparing MUSE data with EAGLE for a Distance Criteria of 7HMR*

2.4 Effect of applying projection and comparing with MUSE observations

For a better comparison to observations, we apply "projection" to our results. We project three dimensional distances in EAGLE into two dimensional distances to calculate the fMM as an observer would. A projected distance of 30kpc on the x-y axes is considered to be a proximity threshold within which two galaxies are classified as potential neighbours. Of these spatial neighbours, those that move within a certain relative velocity in the z-axis (perpendicular to the observer), are taken to be in close pairs or mergers.

Here, we compare the fMM calculated from mergers defined by a projected distance threshold of 30kpc and relative velocities 500km/s and 100 km/s along with the fMM calculated without projection in Fig. 2.8. fMM is plotted versus the median of the redshifts within the redshift bin of binsize of 0.2. We see that the fMM calculated for a merger defined by a relative velocity of 500km/s is higher than the fMM calculated for 100km/s and without projection. Also, the fMM calculated for a merger defined by a relative velocity of 100km/s is greater than for the one defined without projection from redshift zero till two, beyond which this trend reverses. The fMM in each case increases with the increase in redshift.

Further, we compare these trend lines with observation results from MUSE to pick an appropriate relative velocity parameter. This is plotted in Fig. 2.9. We see that the fMM plotted with projection with a relative velocity between the galaxies of 500km/s, agrees best with observations. Thus, henceforth in this thesis we define major mergers as galaxies lying within a projected distance of 30kpc and having a relative velocity within 500km/s.

2.5 Forthcomings

The calculated fMM is not accurate due to the way the number of major pairs are calculated. Two galaxies are considered to be in a major merger if their centre of potentials spatially lie within a pre-defined distance criteria and they have a mass ratio (μ) greater than 1/6. The written algorithm to identify major mergers works in the following manner. Each galaxy with a mass greater than $10^{9.5}$ M$\odot$ is looped over and all the galaxies in the simulation that lies within the pred-defined distance criteria is noted. Of these close neighbours, galaxies with a mass greater than 1/6th its mass are counted as major neighbours. If a major neighbour happens to also be in the mass range of $9.5 < \log_{10} M[M\odot] < 11.5$, it is counted twice, as the looping goes over both galaxies. Therefore, the fMM might be slightly less than what is computed here. This double counting of major mergers was accounted for and the results were compared. There seemed to be very little difference between the two values of fMMs, implying that such a scenario is rare. Hence, the original algorithm is retained for simplification purposes.

Version of June 2018– Created August 1, 2018 - 11:03

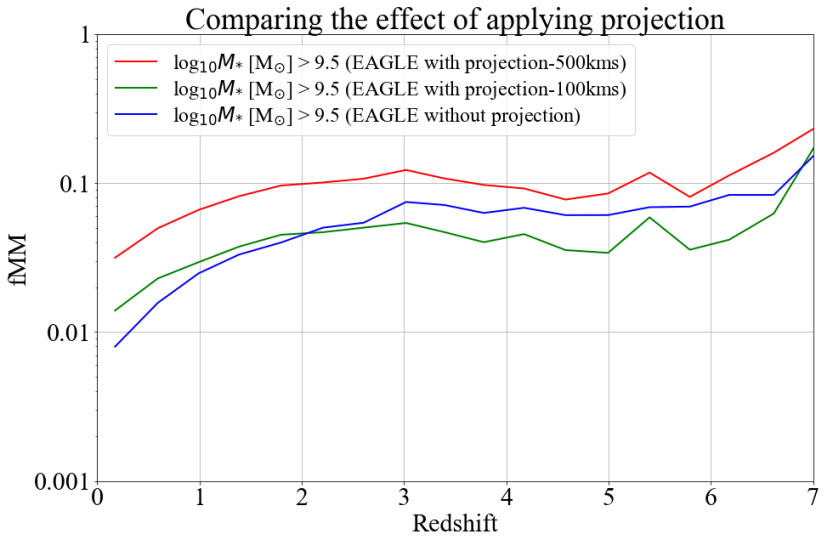

Figure 2.8: *The effect of projection is compared for two threshold velocities 500 and 100 km/s*

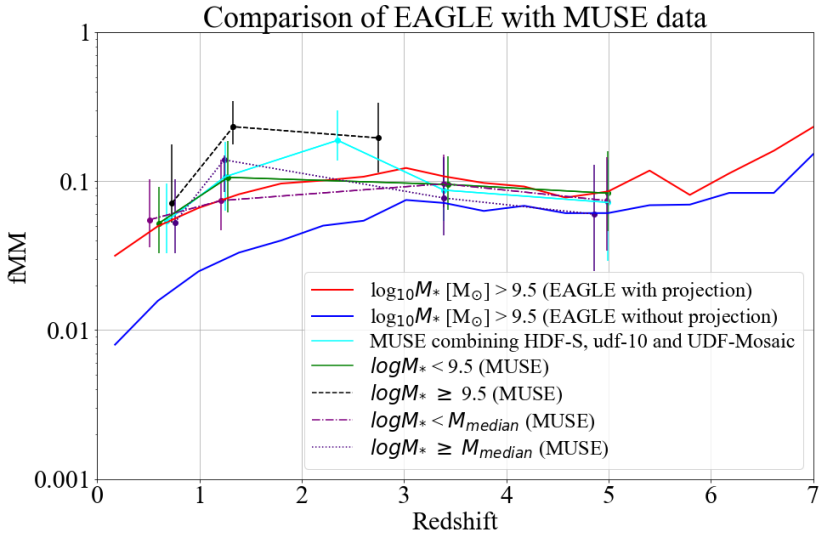

Figure 2.9: *Comparing MUSE data with EAGLE, with and without projection*

Chapter 3

Galaxy morphology and merger history

Galaxies are usually classified based on their visual appearance and are divided into three broad categories namely- ellipticals, spirals and lenticulars. In this chapter, we use the kinematic based parameter kappa and classify the galaxies in EAGLE simulations into two categories, namely ellipticals and disks. We map the morphological distribution of galaxies at redshift zero and analyse its evolution in time. We evaluate the probability of a galaxy undergoing a major merger given its morphology. We also explore the morphological composition of pairs.

3.1 Morphological classification of galaxies

Galaxies in EAGLE simulations have been classified as ellipticals and disks based on their angular momentum (Claudia del P. Lagos et al. 2017). Ellipticals are characterised by a well defined central bulge that comprises stars orbiting in random directions whereas, disks comprises stars rotating along a well defined central flat disk in an orderly manner thus achieving a higher angular momentum than ellipticals.

We quantify galaxy morphology by the parameter kappa-corotating (κ_{corot}), defined as the fraction of the kinetic energy in the stars that move in an ordered rotation along the direction of rotation of the galaxy and lie within 30kpc of the galaxies' centre of potential. κ_{corot} is given as-

$$\kappa_{corot} = \frac{K_{rot}}{K} = \frac{1}{K} \sum_{i}^{r<30kpc} \frac{1}{2} m_i [L_{z,i}/(m_i R_i)]^2 \tag{3.1}$$

where,

$$L_{z,i} = L_i^{along\ \vec{L}=\sum_i^{r<30kpc} L_i}$$

m_i is the mass of each stellar particle and R_i is the projected distance to the axis of rotation $\vec{L}$. $\vec{L}$ and K are the total angular momentum (axis of rotation) and kinetic energy of all the stars lying within 30kpc of the galaxy centre respectively. Of these stars, the angular momentum and kinetic energy of those that are oriented towards the axis of rotation are given by $L_{z,i}$ and K_{rot} respectively.

Thus, the ratio K_{rot}/K (= κ_{corot}) gives the fraction of stars that are in an ordered rotation around the centre and excludes those that are rotating in the opposite direction or haphazardly. In other words, κ_{corot} gives an essence of the diskness of the galaxy.

Therefore, galaxies with a high κ_{corot} are classified as disks, else they are classified as ellipticals. The threshold value of kappa separating ellipticals from disks is taken to be 0.4 as in Correa et al. (2017). This value was obtained from visual inspection of a large number of galaxies. Therefore, galaxies with kappa$\geq$ 0.4 are regarded as disks, else they are classified as ellipticals. This kinematic classification is accurate since we know from the comparisons with the gri-composite images that kinematic morphology can be used as a proxy for visual morphology as confirmed in Correa et al. (2017).

3.2 Distribution of ellipticals and disks at redshift zero for centrals and satellites

Studying the current morphological distribution of galaxies provides insight into the assembly history of galaxies. Once we have identified galaxies from our sample space either as ellipticals or disks, we map the fraction of ellipticals and disks as a function of stellar mass at redshift zero in Fig. 3.1. Here, the fraction of ellipticals and disks are plotted versus the median stellar mass of galaxies within a stellar mass bin of binsize 0.2. We find that the majority of the less massive ($\log_{10}M[M\odot] < 9.75$) and extremely massive ($\log_{10}M[M\odot] > 10.75$) galaxies are mostly ellipticals, whereas, moderately massive ($9.75 < \log_{10}M[M\odot] < 10.75$) galaxies are predominantly disks. The same trend is maintained over centrals and satellites alike.

We find the same trend of galaxy morphology with stellar mass as in Martin et al. (2017) who uses Horizon-AGN simulation and quantifies morphology by the ratio v/σ where v is the 'mean rotational velocity' and σ is the 'mean velocity dispersion'.

Further, we also compare our results with Fig. 4 of Clauwens et al. (2018), that shows kinematic morphology of central galaxies (quantified by spheroid-to-total stellar mass ratio) as a function of stellar mass for several redshifts and finds agreement.

Version of June 2018– Created August 1, 2018 - 11:03

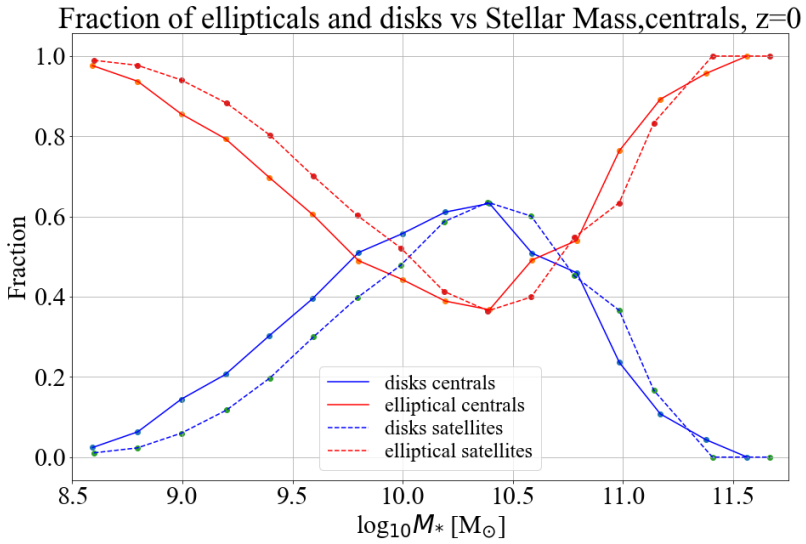

Figure 3.1: *Fraction of ellipticals and disks as a function of stellar mass at redshift zero. The bold and the dashed lines indicate centrals and satellites respectively.*

3.3 Distribution of ellipticals and disks at all redshifts

Once the morphological distribution of galaxies is visualised in several mass bins at redshift zero, as a next step, we attempt to understand their evolution in time. There are several theories about how morphologies assemble.

According to the standard model of galaxy formation, in a cold dark matter universe (ΛCDM), each dark matter halo contains cold gas that condense along a disk forming stars that indulge in an orderly rotation, leading to the formation of a disk-like galaxy with a high angular momentum. As the structures grow hierarchically, mergers are inevitable and these dark matter haloes interact by collisions/mergers. If the galaxy is gas rich, a merger enables star formation in the disk hence retaining its angular momentum and disk like morphology, but otherwise causes dispersion of the disk stellar mass to the halo and the bulge (although proven to be not very efficient- Kannan et al. 2015). This dispersion changes the morphology of a galaxy to more spheroidal like, hence transforming disks to ellipticals/spheroids. (Clauwens et al. 2018, Kannant et al. 2015)

Another theory (Krumholz et al. 2017) states that since galaxies are formed in the intersection of dark matter filaments, during formation, matter is accreted towards the centre causing star formation in the bulge, thus leading to the formation of spheroids without having to undergo any merger events.

To arrive a step closer in understanding the evolution of the morphology of galaxies in EAGLE, we plot the fraction of ellipticals and disks as a function

Version of June 2018– Created August 1, 2018 - 11:03

of redshift in Fig. 3.2. We see that there are more ellipticals than disks at redshift zero. This changes between redshift 0.1 and 1 where disks dominate and beyond redshift 1, ellipticals dominate.

A higher population of ellipticals than disks at higher redshifts ($z > 1$) is contrary to what is anticipated based on the standard model of galaxy formation which predicts the exact opposite. We believe that this result might be due to a resolution effect in the EAGLE simulations. Disks are formed from the balance of the inward gravitational force to the outward pressure from stellar feedback and this balance is not achieved in the EAGLE simulations at higher redshifts due to an insufficient number of stellar particles in galaxies, owing to the simulation's inadequate resolution. Thus, this imbalance renders EAGLE simulations incapable of forming disks at higher redshifts.

However, we find that the plot agrees with Martin et al. (2017) at redshift zero and conclude that most of the stellar mass today lies in early type galaxies.

A similar graph was plotted considering irregular galaxies, where the morphologies were quantified as- (a) ellipticals for a kappa < 0.3, (b) irregulars if they had $0.3 \leq$ kappa < 0.5 and (c) disks if kappa ≥ 0.5. We saw that the irregulars dominated until redshift 1.8 and ellipticals dominated beyond that. Although irregulars were defined, we saw that it did not affect the trend in the distribution of ellipticals and disks.

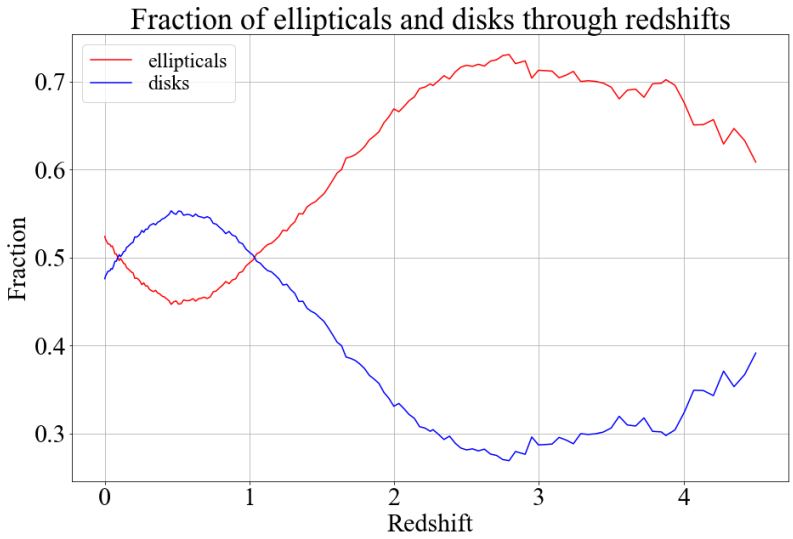

Figure 3.2: *Fraction of ellipticals and disks as a function of redshift is plotted. From the graph we find that there are more ellpiticals than disks at redshift zero. This changes between redshift 0.1 to 1 where disks dominate. Beyond redshift 1, ellipticals dominate.*

Version of June 2018– Created August 1, 2018 - 11:03

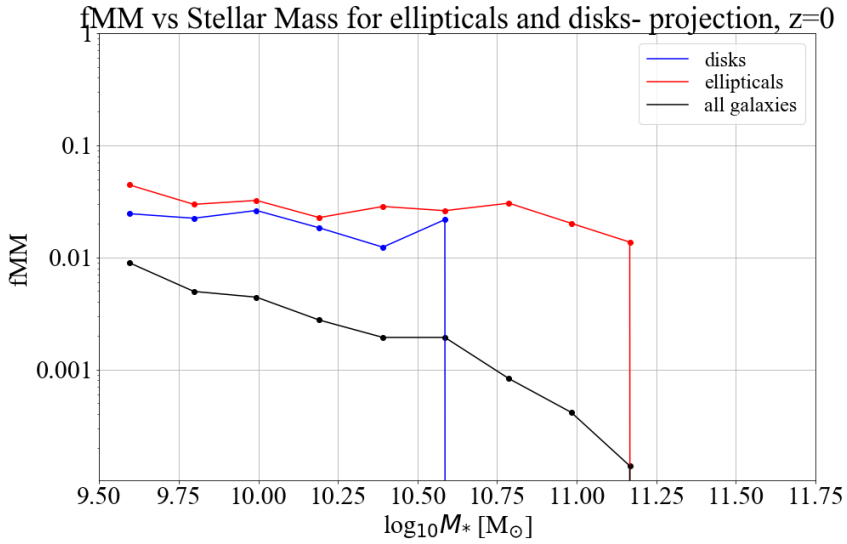

Figure 3.3: *fMM of ellipticals and disks as a function of stellar mass at redshift zero, with projection.*

3.4 Fraction of major mergers at redshift zero

Since we know the morphological distribution of galaxies and their evolution in time, we now attempt to understand their merger histories in terms of their morphologies to pick up any correlation. We calculate the fMM of galaxies separately for ellipticals and disks as shown in the equations below,

$$fMM = \frac{number\ of\ major\ pairs\ in\ a\ mass\ bin}{total\ number\ of\ galaxies\ in\ that\ bin}$$

$$fMMe = \frac{number\ of\ major\ pairs\ of\ ellipticals\ in\ a\ mass\ bin}{total\ number\ of\ ellipticals\ in\ that\ bin}$$

$$fMMd = \frac{number\ of\ major\ pairs\ of\ disks\ in\ a\ mass\ bin}{total\ number\ of\ disks\ in\ that\ bin}$$

We then plot the above calculated fMM versus the median stellar mass of the galaxies in the mass bin with a bin size of 0.2 in Fig. 3.3. We find that at a fixed morphology, fMM is independent of stellar mass and that it is higher for ellipticals than disks at all mass bins.

3.5 Fraction of major mergers as a function of kappa

From Fig. 3.3 we find that the fMM is higher for ellipticals than for disks at all mass bins. To understand this trend further, we plot the fMM as a function of kappa. We also plot this across several redshifts (z= 0 to 2) to find any changes in its trend with time. We plot the fMM versus the median value of kappa of all the galaxies in each kappa bin with a binsize of 0.1. Here, the fraction of major mergers is calculated as,

$$fMM = \frac{number\,of\,major\,pairs\,in\,a\,kappa\,bin}{total\,number\,of\,galaxies\,in\,all\,the\,bins}$$

We see in Fig. 3.4 that the fMM slightly reduces with an increasing kappa, implying that, disks have a lower probability to undergo a major merger event than ellipticals at redshift zero. This trend is seen to be maintained over all redshifts till two. We also see that the fMM is higher for higher redshifts independent of morphology, implying that more mergers occurred at higher redshifts than at current times. This graph is plotted taking into account the effects of projection.

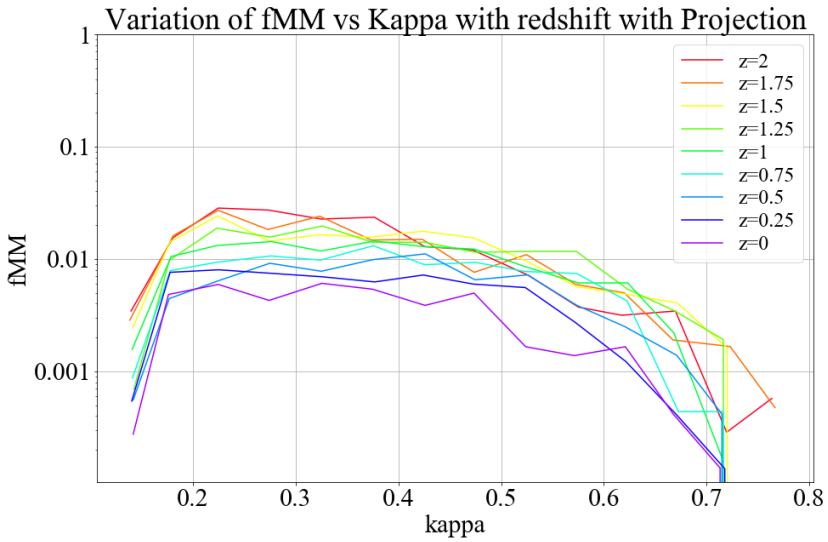

Figure 3.4: *Fraction of major mergers(fMM) is plotted as a function of kappa at redshifts 0-2, with projection. It is observed that the probability of mergers decreases for disk-like galaxies. It is also observed that the probability of mergers is higher at higher redshifts for all morphologies.*

3.6 Fraction of major mergers at all redshifts

We observe in Fig. 3.4 that the fMM increases at higher redshifts independent of morphology. To further understand the evolution of the fMM through time, we plot fMM with a differentiation in morphology as a function of redshift in Fig. 3.5. Here, the fMM are calculated for all galaxies, ellipticals and disks respectively as,

$$fMM = \frac{number\,of\,major\,pairs\,per\,redshift}{total\,number\,of\,galaxies\,in\,that\,redshift}$$

$$fMMe = \frac{number\,of\,major\,pairs\,of\,ellipticals\,per\,redshift}{total\,number\,of\,galaxies\,in\,that\,redshift}$$

$$fMMd = \frac{number\,of\,major\,pairs\,of\,disks\,per\,redshift}{total\,number\,of\,galaxies\,in\,that\,redshift}$$

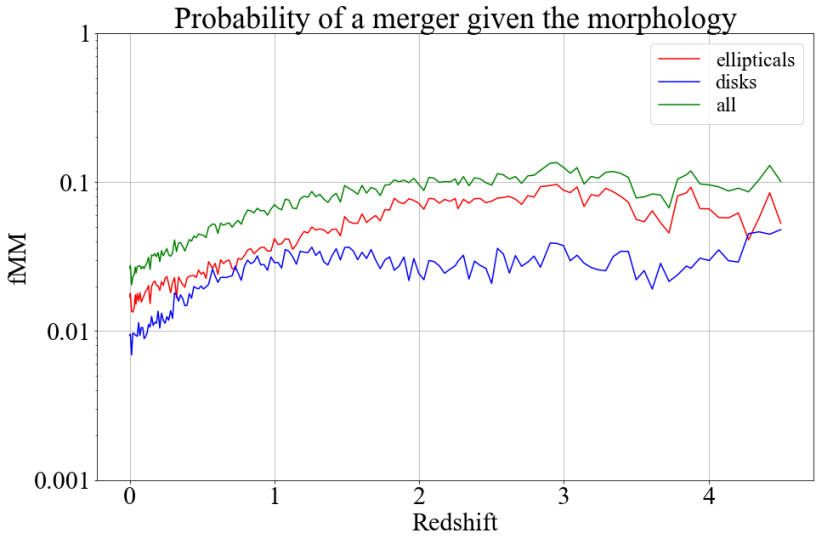

Figure 3.5: *The fMM vs redshift is plotted for ellipticals and disks. We see that the probability of a major merger is higher for ellipticals than for disks.*

From Fig. 3.5 we see that the fMM decreases with decreasing redshift for both ellipticals and disks, implying that the probability of the occurence of a major merger event for either morphologies is decreasing with time. The plot also implies that, it is more probable for ellipticals to experience a merger than for disks over all redshifts.

Given a morphology, the probability of a major merger event calculated above doesn't take into account the fact that there are more ellipticals than disks at higher redshifts as seen in Fig. 3.2. Hence, a normalised probability of a major

Version of June 2018– Created August 1, 2018 - 11:03

merger given a morphology is calculated, where we account for the mis-match in the populations of ellipticals and disks. This provides insight into the innate nature of mergers for each morphology. The normalised fraction of major mergers (fMM) for all galaxies, ellipticals and disks respectively is calculated as,

$$fMM = \frac{number\ of\ major\ pairs\ per\ redshift}{total\ number\ of\ galaxies\ in\ that\ redshift}$$

$$fMMe = \frac{number\ of\ major\ pairs\ of\ ellipticals\ per\ redshift}{total\ number\ of\ ellipticals\ in\ that\ redshift}$$

$$fMMd = \frac{number\ of\ major\ pairs\ of\ disks\ per\ redshift}{total\ number\ of\ disks\ in\ that\ redshift}$$

The normalised probability of major mergers given a morphology, is plotted as a function of redshift in Fig. 3.6. It is observed that the normalised probability for a major merger is still higher for ellipticals than disks from redshift zero to around two. From Fig. 3.2 we know that disks dominate from redshift 0.1 to 1, but its normalised probability for undergoing a major merger is almost two times lower than that of ellipticals in the same redshift range. This implies that disks are more isolated than ellipticals between redshifts 0.1 and 1. Also, just as in the previous case, the overall trend of the normalised fMM increases with the increase in redshift for either morphologies.

Figure 3.6: *The normalised probability of a major merger is plotted for ellipticals and disks. It is seen that the probability of a major merger is higher for ellipticals than for disks until around redshift two, implying that disks might be more isolated than ellipticals between redshift 0.1 to 1.*

Version of June 2018– Created August 1, 2018 - 11:03

From all the previous plots, we find that the fMM for ellipticals and disks per redshift is lower than 0.1. This implies that, the probability of galaxies undergoing a merger is low per redshift, but mergers are believed to be one of the major causes of interaction between galaxies that help shape their evolution. Thus to verify this, we calculate the cumulative probability of major mergers per morphology through redshifts and plot it in Fig. 3.7. We find that, between redshifts zero to five, galaxies undergo close to six mergers where, ellipticals undergo four and disks undergo two mergers. From these values we conclude that mergers are extremely rare in the universe and might not be entirely responsible for the morphological transformation of galaxies.

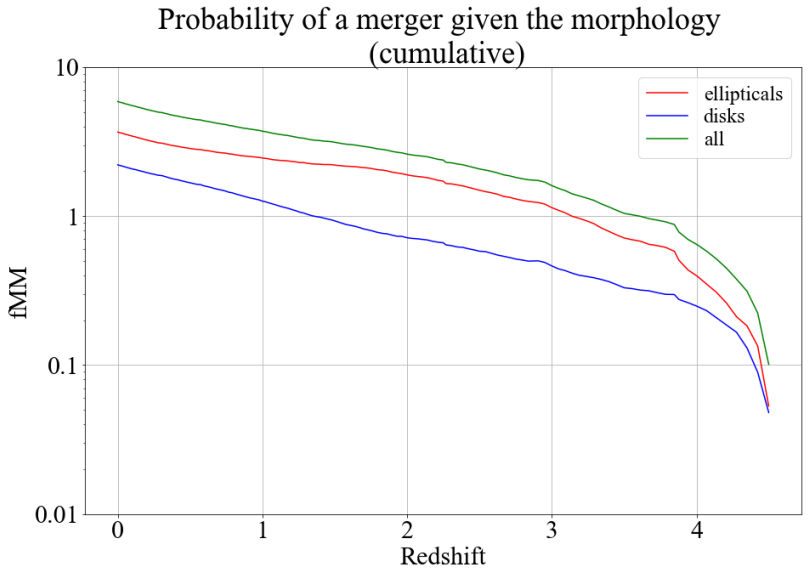

Figure 3.7: *Cumulative probability of a merger given the morphology is plotted here. We see that ellipticals undergo a total of four mergers whereas disks undergo two mergers across all redshifts, implying that mergers are rare and might not be entirely responsible for the morphological transformation of galaxies.*

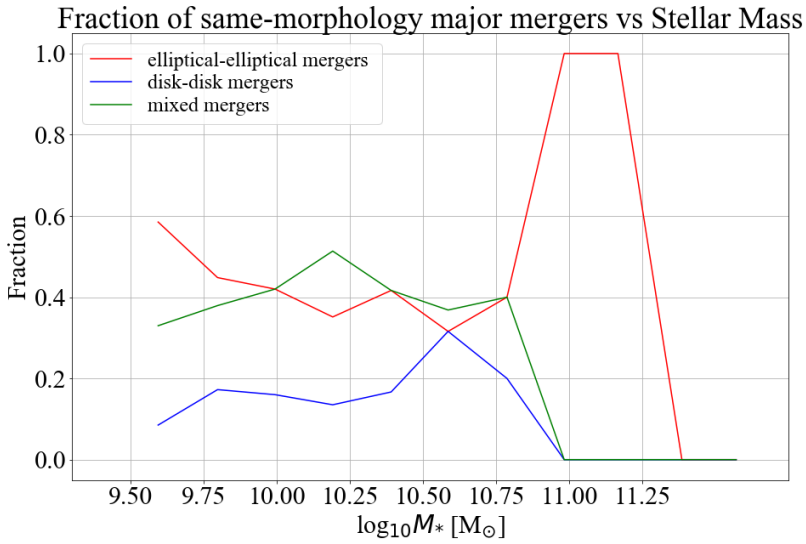

Figure 3.8: *Mass distribution of same-morphology major mergers at redshift zero.This gives us an idea about the population of pairs at redshift zero.*

3.7 Major mergers between galaxies with same morphology at redshift zero

We explore the environment of the elliptical and disk galaxies undergoing mergers by looking at what comprises the pairs. We count the number of close pairs, determine how many of those are elliptical-elliptical, disk-disk and mixed and plot the fraction of their population as a function of stellar mass in Fig. 3.8. This gives us an idea about the population distribution of pairs with different morphologies at redshift zero.

We also plot the fMM of the same morphology major pairs across stellar mass at redshift zero in Fig. 3.9. The fMM is plotted versus the median stellar mass of galaxies in the mass bin with a binsize of 0.2. This gives us an idea about the population distribution of pairs with different morphologies relative to the total number of galaxies. Here, the fMM for all galaxies, elliptical, disk and mixed pairs are calculated respectively as,

$$fMM = \frac{number\ of\ major\ pairs}{total\ number\ of\ galaxies\ in\ each\ bin}$$

$$fMMe = \frac{number\ of\ major\ elliptical - elliptical\ pairs}{total\ number\ of\ galaxies\ in\ each\ bin}$$

$$fMMd = \frac{number\ of\ major\ disk - disk\ pairs}{total\ number\ of\ galaxies\ in\ each\ bin}$$

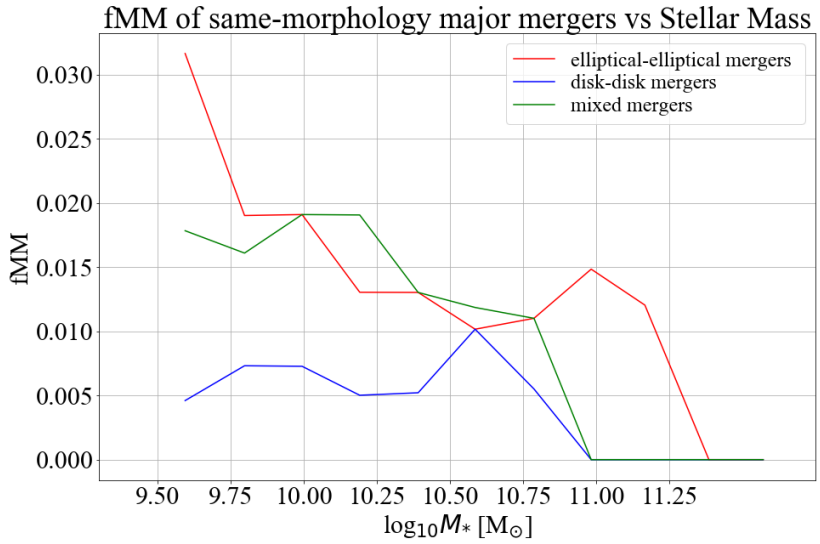

Figure 3.9: *The fraction of same- morphology major mergers is plotted at redshift zero. This gives us an idea about the population of pairs relative to the total number of galaxies. It is seen that the fMM is higher for ellipticals than for disks implying that it is more probable to see two elliptical galaxies in a major merger than two disk galaxies.*

$$fMMm = \frac{number\,of\,major\,mixed\,pairs}{total\,number\,of\,galaxies\,in\,each\,bin}$$

We find that the fMM is higher for ellipticals than for disks, which implies that at redshift zero, it is more probable to see two elliptical galaxies in a major merger than two disk galaxies, independent of their stellar mass. It is also seen that the probability of finding a mixed merger is high for galaxies in the mass range $10 \leq \log_{10}M[M\odot] \leq 10.75$. This can be owed to the higher number of disks in the same mass range as seen from Fig. 3.1. Thus, we conclude that the elliptical galaxies are involved in the majority of mergers independent of stellar mass at redshift zero.

3.8 Same morphology galaxies experiencing major mergers at all redshifts

It is seen from Fig. 3.9 that at redshift zero, the ellipticals are more likely to be found in pairs with other ellipticals over all stellar mass bins. To understand how this has evolved through time, the fMM of the same morphology major pairs is plotted across redshifts in Fig. 3.10. Here, the fMM for all galaxies, elliptical, disk and mixed pairs are calculated respectively as,

$$fMM = \frac{number\ of\ major\ pairs\ per\ redshift}{total\ number\ of\ galaxies\ in\ that\ redshift}$$

$$fMMe = \frac{number\ of\ major\ elliptical-elliptical\ pairs\ per\ redshift}{total\ number\ of\ galaxies\ in\ that\ redshift}$$

$$fMMd = \frac{number\ of\ major\ disk-disk\ pairs\ per\ redshift}{total\ number\ of\ galaxies\ in\ that\ redshift}$$

$$fMMm = \frac{number\ of\ major\ mixed\ pairs\ per\ redshift}{total\ number\ of\ galaxies\ in\ that\ redshift}$$

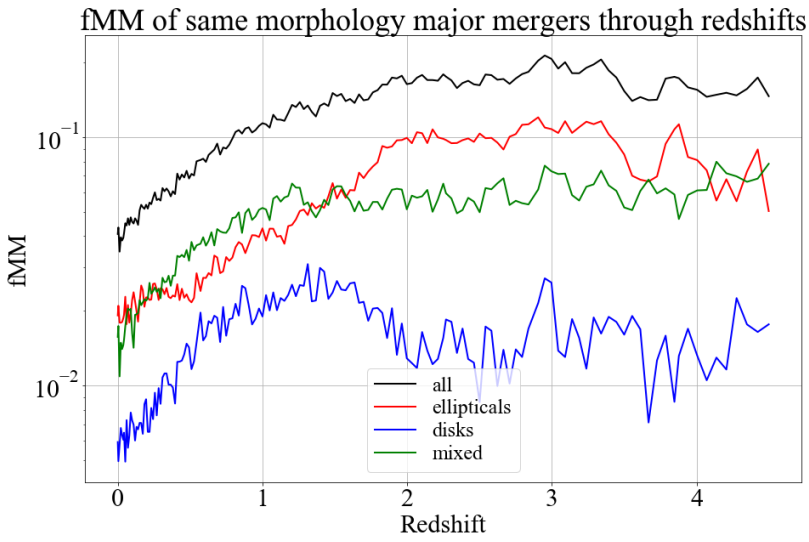

Figure 3.10: *Fraction of same-morphology major mergers(fMM) at all redshifts.*

It is seen from Fig. 3.10 that the probability of mergers of elliptical galaxies is higher than disks across all redshifts which implies that elliptical-elliptical mergers are more common than disk-disk mergers across all redshifts. This is compared with the Fig. 5 of Martin et al. (2017). The paper explores the morphologies of the progenitors of early-type (elliptical) galaxies today that are involved in mergers. The plot shows that the mergers involve at least one late-type (disk) galaxies throughout all redshifts with the early-type mergers dominating only at recent redshifts. This is contradictory to what we found as seen in Fig. 3.10. Also, the probability of mixed mergers are more than disk-disk mergers at all redshifts, implying that major mergers usually involve at-least one elliptical galaxy at all redshifts. This contradiction might exist because the paper considers only the progenitors of local early-type mergers, whereas here all morphologies are considered. It can also be due to the resolution effect of EAGLE that reduces the number of disks at higher redshifts.

Version of June 2018– Created August 1, 2018 - 11:03

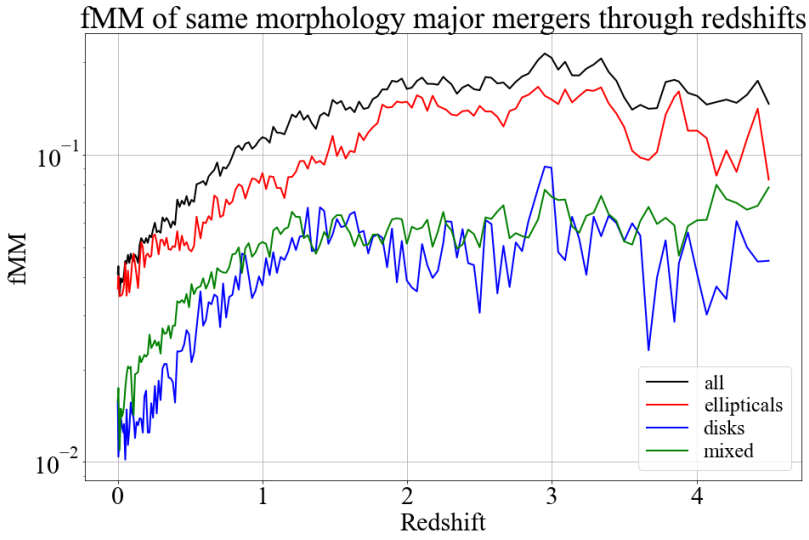

Figure 3.11: *Normalised fraction of same-morphology major mergers(fMM) at all redshifts is plotted here. It is observed that this fraction is higher for elliptical mergers than disks. The graph also plots the evolution of mixed and all mergers with redshift.*

As in the previous section, the above results can be normalised by accounting for the population of ellipticals and disks. This will help us understand the nature of mergers for ellipticals and disks and provides a deeper insight into the environment of these galaxies. Normalised fraction of same morphology major mergers for all galaxies, elliptical, disk and mixed pairs plotted in Fig. 3.11 are calculated respectively as,

$$fMM = \frac{number\,of\,major\,pairs\,per\,redshift}{total\,number\,of\,galaxies\,in\,that\,redshift}$$

$$fMMe = \frac{number\,of\,major\,elliptical-elliptical\,pairs\,per\,redshift}{total\,number\,of\,ellipticals\,in\,that\,redshift}$$

$$fMMd = \frac{number\,of\,major\,disk-disk\,pairs\,per\,redshift}{total\,number\,of\,disks\,in\,that\,redshift}$$

$$fMMm = \frac{number\,of\,major\,mixed\,pairs\,per\,redshift}{total\,number\,of\,galaxies\,in\,that\,redshift}$$

We see that, the normalised fraction of same morphology major mergers is higher for ellipticals than disks implying that, it is more probable to find elliptical galaxies in a merger than disks across all redshifts. The overall probability due to normalisation increases but the trend remains the same. Hence, we can conclude that the probability of finding ellipticals in mergers is always more than disks across all redshifts.

Chapter 4

Conclusion

In this thesis we investigate the link between merger histories and morphology of galaxies in the EAGLE simulations. We attempt to assess the significance of mergers (major) in shaping the galaxy evolution by quantifying how often they occur. We count the number of major merger pairs relative to the galaxy population per redshift, and define it as the 'fraction of major mergers' or fMM. fMM depends on how major mergers are defined which are inturn defined by a specific distance and mass criteria (μ (Mu) = M_2/M_1 where $M_1 > M_2$). We define the mass criteria as $\mu \geq 1/6$, and compare several values of distance criteria to arrive at the appropriate value. We see that, a distance criteria of 30kpc fits best with observation results from MUSE (Ventou et al. 2016). Also we see that, the fMM defined this way is independent of stellar mass. For a better comparison with observations, we apply projection. This way we plot our results just as an observer would. We see that fMM continuously increases with an increase in redshift, implying that major merger events were more common in the past than at the present time.

It is believed that mergers affect various galactic properties. Hence we attempt to understand the link between morphology of galaxies and mergers in the EAGLE simulation. We start by morphologically classifying our sample of galaxies into disks and ellipticals, based on the fraction of angular momentum of the stars in the galaxy that are invested in orderly circular rotation along the direction of galaxy rotation, here κ_{corot}. A higher value of the fraction κ_{corot} implies a disk-like morphology whereas a lower value implies an elliptical morphology. We map the distribution of the morphology at redshift zero and its evolution through time. We see that elliptical galaxies comprise the low ($\log_{10}M[M\odot] < 9.75$) and high ($\log_{10}M[M\odot] > 10.75$) mass regime whereas most disk galaxies are moderately massive ($9.75 < \log_{10}M[M\odot] < 10.75$). We also see that this trend is followed by centrals and satellites alike. Several works in literature have been quoted to corroborate our results.

We map the ellipticals and disks in time and discern that there are more ellipticals than disks at redshift zero till redshift 0.1. This trend reverses between redshift 0.1 to 1 where the disks dominate. Beyond 0.1 there are more ellipticals

than disks at all higher redshifts. We gather that this result is not conclusive since it might be a resolution effect of the EAGLE simulations.

We calculate the fMM for each morphology and find that at a fixed morphology, the fMM is independent of stellar mass. We also find that fMM decreases with the increase in κ_{corot} at redshift zero implying that fMM is higher for ellipticals than for disks. We quantify the probability of undergoing a major merger given a morphology and find that the probability of undergoing a major merger is higher for ellipticals than disks by almost two times across all redshifts. We remove the influence of the unmatched population of each morphology on fMM by normalising it. We see that the normalised probability is still higher for ellipticals than for disks until redshift two, implying that ellipticals have a higher tendency of mergers than disks. We deduce from a higher disk population between redshift 0.1 to 1 and a lower probability of major mergers for the same at that range that, disks are more isolated than ellipticals. We also calculate the cumulative fMM and find that elliptical galaxies undergo four mergers whereas disks undergo two mergers from redshift six to zero. This also implies that mergers are very rare in the Universe and hence might not entirely be responsible for the morphological transformation of galaxies.

Further, we study the morphologies of galaxies comprising the pairs. We see that it is more likely to find two ellipticals merging than mixed mergers or two disks across all redshifts in the same order. Normalising the probability to account for the unmatched population of ellipticals and disks does not change this trend.

Chapter 5

Future work

Mergers are believed to impact galactic properties like morphology, mass and size. In this thesis, we have explored the link between merger histories of galaxies and their morphology in the EAGLE simulations. Further on, we can explore its impact on the mass and size of the galaxies involved, by following individual galaxies and their merger events in time through all the EAGLE snapshots. We can strive towards understanding the correlation between star formation rate and mergers, as it is believed that mergers trigger star formation and lastly, we can calculate the local densities of ellipticals and disks separately to corroborate the claim that ellipticals exist in denser environments than disks.

Appendix A

Appendix

Distance Criteria - The proximity threshold between two galaxies to be regarded as neighbours.

Fraction of major mergers (fMM) - The ratio of the number of pairs to the total number of galaxies in the sample space considered.

κ_{corot} - The fraction of the kinetic energy invested in stars in orderly rotation indicative of the galaxy morphology.

Major Mergers - Galaxy pairs that lie within a distance of 30kpc from each others' centre of potential and have a mass ratio (μ = M_2/M_1 where $M_1 > M_2$) greater than $1/6$.

Mass Criteria - The ratio of the masses of the two galaxies involved in a merger to be regarded as a major merger.

Stellar Mass - The total mass of all the stars in a galaxy lying within a 30kpc radius from its centre of potential in the EAGLE simulations.

Acknowledgements

I would like to thank my first supervisor Dr. Joop Schaye for this opportunity of working on this project. I would also like to thank my second supervisor Dr. Camila Correa for her constant guidance in this thesis. I not only learned a lot but also thoroughly enjoyed doing so. Her continuous involvement throughout the project and innumerable corrections to the report has led me to complete this thesis. I would like to thank the second reader for taking the time to read my thesis and giving valuable comments on it.

Finally, I would like to express my gratitude to my parents, friends and classmates for their constant support. Master thesis can be stressful and I would like to thank my boyfriend for making it easier for me.

Bibliography

[1] Clauwens, B., J. Schaye, M. Franx, and R. G. Bower
2018. The three phases of galaxy formation. *Monthly Notices of the Royal Astronomical Society*, 478(3):3994–4009.

[2] Conselice, C. J.
2014. The evolution of galaxy structure over cosmic time. *Annual Review of Astronomy and Astrophysics*, 52(1):291–337.

[3] Correa, C. A., J. Schaye, B. Clauwens, R. G. Bower, R. A. Crain, M. Schaller, T. Theuns, and A. C. R. Thob
2017. The relation between galaxy morphology and colour in the eagle simulation. *Monthly Notices of the Royal Astronomical Society: Letters*, 472(1):L45–L49.

[4] Fall, S. M. and G. Efstathiou
1980. Formation and rotation of disc galaxies with haloes. *Monthly Notices of the Royal Astronomical Society*, 193(2):189–206.

[5] Fontanot, F., A. V. Macció, M. Hirschmann, G. De Lucia, R. Kannan, R. S. Somerville, and D. Wilman
2015. On the dependence of galaxy morphologies on galaxy mergers. *Monthly Notices of the Royal Astronomical Society*, 451(3):2968–2977.

[6] Hopkins, P. F.
2008. Quenching Models: Their Interplay and Degeneracies. In *Panoramic Views of Galaxy Formation and Evolution*, T. Kodama, T. Yamada, and K. Aoki, eds., volume 399 of *Astronomical Society of the Pacific Conference Series*, P. 405.

[7] Kannan, R., A. V. Macció, F. Fontanot, B. P. Moster, W. Karman, and R. S. Somerville
2015. From discs to bulges: effect of mergers on the morphology of galaxies. *Monthly Notices of the Royal Astronomical Society*, 452(4):4347–4360.

[8] Krumholz, M. R., B. Burkhart, J. C. Forbes, and R. M. Crocker
2018. A unified model for galactic discs: star formation, turbulence driving, and mass transport. *Monthly Notices of the Royal Astronomical Society*, 477(2):2716–2740.

[9] Lagos, C., A. R. H. Stevens, R. G. Bower, T. A. Davis, S. Contreras, N. D. Padilla, D. Obreschkow, D. Croton, J. Trayford, C. Welker, and T. Theuns
2017. The catastrophic effect of mergers on the angular momentum and morphology of galaxies in eagle.

[10] Madau, P. and M. Dickinson
2014. Cosmic star-formation history. *Annual Review of Astronomy and Astrophysics*, 52(1):415–486.

[11] Mantha, K. B., D. H. McIntosh, R. Brennan, H. C. Ferguson, D. Kodra, J. A. Newman, M. Rafelski, R. S. Somerville, C. J. Conselice, J. S. Cook, N. P. Hathi, D. C. Koo, J. M. Lotz, B. D. Simmons, A. N. Straughn, G. F. Snyder, S. Wuyts, E. F. Bell, A. Dekel, J. Kartaltepe, D. D. Kocevski, A. M. Koekemoer, S.-K. Lee, R. A. Lucas, C. Pacifici, M. A. Peth, G. Barro, T. Dahlen, S. L. Finkelstein, A. Fontana, A. Galametz, N. A. Grogin, Y. Guo, B. Mobasher, H. Nayyeri, P. G. PÃ©rez-GonzÃ¡lez, J. Pforr, P. Santini, M. Stefanon, and T. Wiklind
2018. Major merging history in candels. i. evolution of the incidence of massive galaxyâgalaxy pairs from zÂ =Â 3 to zÂ âŒÂ 0. *Monthly Notices of the Royal Astronomical Society*, 475(2):1549–1573.

[12] Martin, G., S. Kaviraj, J. E. G. Devriendt, Y. Dubois, C. Pichon, and C. Laigle
2018. Identifying the progenitors of present-day early-type galaxies in observational surveys: correcting âprogenitor biasâ using the horizon-agn simulation. *Monthly Notices of the Royal Astronomical Society*, 474(3):3140–3151.

[13] McAlpine, S., J. Helly, M. Schaller, J. Trayford, Y. Qu, M. Furlong, R. Bower, R. Crain, J. Schaye, T. Theuns, C. D. Vecchia, C. Frenk, I. McCarthy, A. Jenkins, Y. Rosas-Guevara, S. White, M. Baes, P. Camps, and G. Lemson
2016. The eagle simulations of galaxy formation: Public release of halo and galaxy catalogues. *Astronomy and Computing*, 15:72 – 89.

[14] Mo, H. J., S. Mao, and S. D. M. White
1998. The formation of galactic discs. *Monthly Notices of the Royal Astronomical Society*, 295(2):319–336.

[15] Qu, Y., J. C. Helly, R. G. Bower, T. Theuns, R. A. Crain, C. S. Frenk, M. Furlong, S. McAlpine, M. Schaller, J. Schaye, and S. D. M. White
2017. A chronicle of galaxy mass assembly in the eagle simulation. *Monthly Notices of the Royal Astronomical Society*, 464(2):1659–1675.

[16] Rodriguez-Gomez, V., L. V. Sales, S. Genel, A. Pillepich, J. Zjupa, D. Nelson, B. Griffen, P. Torrey, G. F. Snyder, M. Vogelsberger, V. Springel, C.-P. Ma, and L. Hernquist
2017. The role of mergers and halo spin in shaping galaxy morphology. *Monthly Notices of the Royal Astronomical Society*, 467(3):3083–3098.

[17] Springel, V.
2005. The cosmological simulation code gadget-2. *Monthly Notices of the Royal Astronomical Society*, 364(4):1105–1134.

[18] Springel, V., J. Wang, M. Vogelsberger, A. Ludlow, A. Jenkins, A. Helmi, J. F. Navarro, C. S. Frenk, and S. D. M. White
2008. The aquarius project: the subhaloes of galactic haloes. *Monthly Notices of the Royal Astronomical Society*, 391(4):1685–1711.

[19] The EAGLE team
2017. The EAGLE simulations of galaxy formation: Public release of particle data. *ArXiv e-prints*.

[20] Tonnesen, S. and R. Cen
2012. Effects on galaxy evolution: pair interactions versus environment. *Monthly Notices of the Royal Astronomical Society*, 425(3):2313–2334.

[21] Toomre, A.
1977. Theories of spiral structure. *Annual Review of Astronomy and Astrophysics*, 15(1):437–478.

[22] Trayford, J. W., C. S. Frenk, T. Theuns, J. Schaye, and C. Correa
2018. The star formation rate and stellar content contributions of morphological components in the EAGLE simulations. *ArXiv e-prints*.

[23] Ventou, E., T. Contini, N. Bouché, B. Epinat, J. Brinchmann, R. Bacon, H. Inami, D. Lam, A. Drake, T. Garel, L. Michel-Dansac, R. Pello, M. Steinmetz, P. M. Weilbacher, L. Wisotzki, and M. Carollo
2017. The MUSE Hubble Ultra Deep Field Survey. IX. Evolution of galaxy merger fraction since z 6. , 608:A9.

[24] Weigel, A. K., K. Schawinski, N. Caplar, A. Carpineti, R. E. Hart, S. Kaviraj, W. C. Keel, S. J. Kruk, C. J. Lintott, R. C. Nichol, B. D. Simmons, and R. J. Smethurst
2017. Galaxy zoo: Major galaxy mergers are not a significant quenching pathway. *The Astrophysical Journal*, 845(2):145.